EPJ Web of Conferences **276**, 01006 (2023) https://doi.org/10.1051/epjconf/202327601006
SQM 2022

Seventh and eighth-order cumulants of net-proton multiplicity distributions in heavy-ion collisions at RHIC-STAR

Ashish Pandav (for the STAR Collaboration)[1,2,*]

[1]School of Physical Sciences, National Institute of Science Education and Research, Jatni 752050, India
[2]Homi Bhabha National Institute, Training School Complex, Anushaktinagar, Mumbai 400094, India

Abstract. We report the first measurements of seventh and eighth-order cumulants of net-proton distributions in Au+Au collisions at $\sqrt{s_{NN}}$ = 27, 54.4, and 200 GeV. The measurements are performed at mid-rapidity $|y| < 0.5$ within $0.4 < p_T < 2.0$ GeV/c using the Time Projection Chamber and Time-of-Flight detector. Motivation for the measurements comes from lattice-QCD and QCD based model calculations that predict their negative signs for a crossover quark-hadron transition. While 0-40% centrality measurements at $\sqrt{s_{NN}}$ = 54.4 and 200 GeV are consistent with zero within large uncertainties, at $\sqrt{s_{NN}}$ = 27 GeV, they are negative with $\leq 1.4\sigma$ significance. The peripheral 70-80% measurements are either positive or consistent with zero for the three energies.

1 Introduction

The phase diagram of strongly interacting matter is called as the Quantum-Chromo-Dynamics (QCD) phase diagram [1]. It has at least two distinct phases: hadronic phase where quarks and gluons are confined within hadrons and the quark-gluon plasma (QGP) phase where they are deconfined. The transition between the two phases at vanishing baryonic chemical potential (μ_B) is shown to be a smooth crossover by first-principle lattice QCD calculations [2]. At large μ_B, several QCD-based model calculations indicate a first-order phase transition terminating at a QCD critical point [3, 4]. Experimental exploration of the QCD phase diagram forms one of the primary goals of the heavy-ion collision experiments. Higher-order cumulants of event-by-event net-particle distributions have been suggested as sensitive observables in this regard [5, 6]. Ratio of the measured cumulants are constructed to eliminate the system volume dependence and facilitate a direct comparison with ratio of susceptibilities (χ_n) calculated from lattice QCD, QCD-based models, and thermal models [7, 8].

The STAR experiment at RHIC has measured cumulants (C_n) of net-proton (as a proxy for net-baryon) distributions up to sixth-order in Au+Au collisions from $\sqrt{s_{NN}} = 3 - 200$ GeV [9–13]. A non-monotonic collision energy dependence of net-proton cumulant ratio C_4/C_2 was observed, which is consistent with a model calculation that includes a critical point [9]. Furthermore, the net-proton C_6/C_2 shows an increasingly negative sign with decreasing collision energy in the range of $\sqrt{s_{NN}} = 7.7 - 200$ GeV [13]. The negative values, albeit with large uncertainties, and the energy dependence are consistent with lattice QCD calculation ($\mu_B < 110$ MeV) that includes a crossover quark-hadron transition [6].

*e-mail: ashish.pandav@niser.ac.in

The study presented in these proceedings extends the net-proton cumulant measurements to even higher orders, i.e. C_7/C_1 and C_8/C_2. The lattice-QCD and various QCD-based models predict negative seventh and eighth-order net-baryon susceptibilities for a crossover quark-hadron transition at vanishing baryonic chemical potential near the transition temperature $T = T_{pc}$ with larger magnitude compared to those at fifth- and sixth-orders [6, 14, 15]. Calculations from a model, called the Polyakov-loop extended quark-meson (PQM) model [15], presented in Fig 1 shows that χ_8^B is an order more negative than χ_6^B at $T = T_{pc}$ for vanishing chemical potential ($\mu_q \sim 0$). In addition to search for crossover in QCD phase diagram, net-proton cumulant ratios C_7/C_1 and C_8/C_2 can also be used to study the validity of hadron resonance gas (HRG) models: Canonical Ensemble (CE) vs. the Grand Canonical Ensemble (GCE) frameworks. In the CE approach [16], the cumulant ratios show a departure from unity and a strong collision energy dependence as compared to GCE [6], where they are unity across all collision energies.

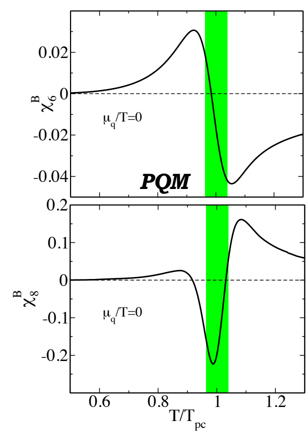

Figure 1. χ_6^B and χ_8^B from the PQM model as a function of T/T_{pc} [15].

2 Analysis Details

Data from Au+Au collisions at $\sqrt{s_{NN}} = 27$ (year 2018), 54.4, and 200 GeV recorded by the STAR detector were analysed. The number of minimum bias events for $\sqrt{s_{NN}} = 27$, 54.4, and 200 GeV are around 300, 550, and 900 millions, respectively. The detectors used for (anti-)proton identification are the Time-Projection-Chamber (TPC) and Time-of-Flight (TOF). The charged particle multiplicity in the psuedo-rapidity (η) range $|\eta| < 1$ excluding protons and anti-protons were used to define centrality to avoid self-correlation effects. The (anti-)protons at mid-rapidity ($|y| < 0.5$) within the transverse momentum (p_T) coverage of $0.4 < p_T < 2.0$ GeV/c were used for measurements. In the p_T range of $0.4 < p_T < 0.8$ GeV/c, only the TPC was used to select (anti-)protons whereas both TPC and TOF were required for (anti-)proton identification in the higher momentum region. To suppress the effect of initial system volume fluctuations on cumulants, Centrality-Bin-Width-Correction (CBWC) was applied [17]. To correct the cumulants for finite detection efficiency, an analytical correction was performed where the detector response was assumed to follow binomial distribution [18]. For estimating statistical uncertainties, bootstrap method was used [19, 20]. Systematic uncertainties on the measurements were estimated varying tracking efficiency, track selection, and particle identification criteria.

3 Results

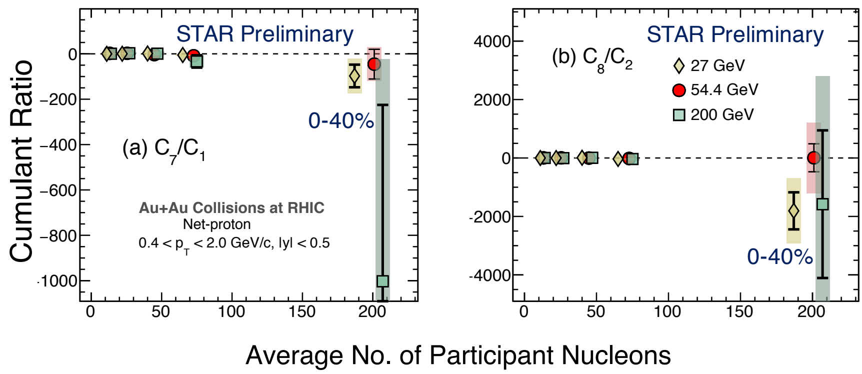

Figure 2. C_7/C_1 (a) and C_8/C_2 (b) of net-proton distributions in Au+Au collisions at $\sqrt{s_{NN}} = 27$ (diamonds), 54.4 (circles), and 200 GeV (squares) as a function of average number of participant nucleons. The bars and shaded bands on the data points represent the statistical and systematic uncertainties, respectively. Results from 70-80%, 60-70%, 50-60%, 40-50%, and 0-40% centrality bins are presented (from left to right).

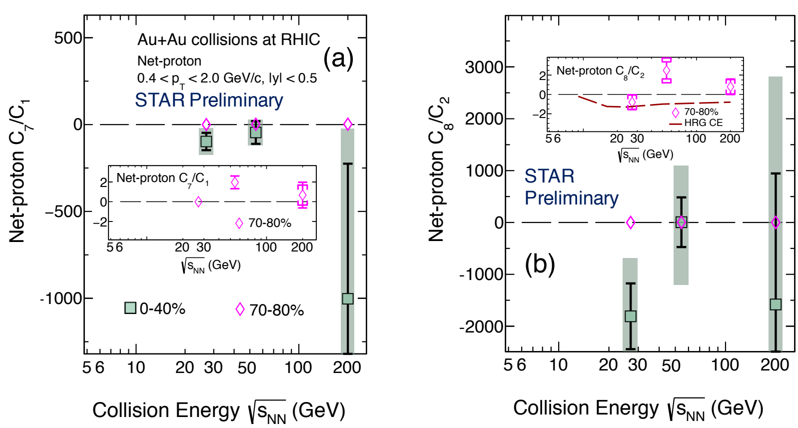

Figure 3. C_7/C_1 (a) and C_8/C_2 (b) of net-proton distributions from Au+Au collisions as a function of collision energy. The results for two centrality bins, 0-40% (filled squares) and 70-80% (open diamonds), are presented. The bars represent the statistical uncertainties. The shaded bands on 0-40% data points and caps on the 70-80% data represent systematic uncertainties. Insets are added in both panel containing peripheral 70-80% data for better visibility. The HRG CE calculations for C_8/C_2 [16] are also shown.

The collison centrality dependence of net-proton C_7/C_1 and C_8/C_2 for $\sqrt{s_{NN}} = 27$, 54.4, and 200 GeV is presented in Fig. 2. A weak dependence on collision centrality is observed within large uncertainties. Larger width of net-proton distributions at $\sqrt{s_{NN}} = 200$ GeV contributes to larger statistical uncertainties at 200 GeV as compared to other two energies. The cumulant ratios for 0-40% centrality at $\sqrt{s_{NN}} = 54.4$ and 200 GeV are consistent with zero within uncertainties. At $\sqrt{s_{NN}} = 27$ GeV, the results for 0-40% centrality are negative with a significance of $\leq 1.4\sigma$ (where σ is the quadrature sum of statistical and systematic uncertainties). The peripheral data, as seen more clearly in Fig. 3, are close to zero.

The energy dependence of net-proton C_7/C_1 and C_8/C_2 for 0-40% and 70-80% centralities are presented in Fig. 3. Within large uncertainties, no clear energy dependence could be observed for the 0-40% measurements. The peripheral data are found to be either positive or consistent with zero within uncertainties.

4 Summary

In summary, we presented the first measurements on seventh and eighth-order net-proton cumulant ratios: C_7/C_1 and C_8/C_2 in Au+Au collisions at $\sqrt{s_{NN}}$ = 27, 54.4, and 200 GeV. While lattice QCD and QCD-based model predicted negative sign of these observables for a smooth crossover, the experimental data at $\sqrt{s_{NN}}$ = 54.4 and 200 GeV are consistent with zero for central 0-40% collisions within large uncertainties. Both the cumulant ratios (for 0-40%) at 27 GeV deviate from unity and show negative values at a significance of $\leq 1.4\sigma$. The peripheral 70-80% data are either positive or consistent with zero for all the energies presented. Measurements in the lower collision energies from the upcoming high statistic BES-II data [21] will be interesting. In addition, $\sim$ 20 billion Au+Au minimum bias collision events at $\sqrt{s_{NN}}$ = 200 GeV which are scheduled to be collected at STAR in the year 2023+2025 [22], will greatly enhance the statistical precision of the measurements.

References

[1] A. Pandav, D. Mallick and B. Mohanty, Prog. Part. Nucl. Phys. **125** (2022), 103960
[2] Y. Aoki, G. Endrodi, Z. Fodor, S. D. Katz and K. K. Szabo, Nature **443**, 675-678 (2006)
[3] S. Ejiri, Phys. Rev. D **78**, 074507 (2008)
[4] E. S. Bowman and J. I. Kapusta, Phys. Rev. C **79**, 015202 (2009)
[5] M. A. Stephanov, Phys. Rev. Lett. 107, 052301 (2011).
[6] A. Bazavov, *et al.* Phys. Rev. D **101**, no.7, 074502 (2020)
[7] S. Gupta, X. Luo, B. Mohanty, H. G. Ritter and N. Xu, Science **332**, 1525 (2011)
[8] F. Karsch and K. Redlich, Phys. Lett. B **695**, 136-142 (2011)
[9] J. Adam et al. *et al.* [STAR], Phys. Rev. Lett. **126**, 092301 (2021)
[10] M. Abdallah *et al.* [STAR], Phys. Rev. C **104**, no.2, 024902 (2021)
[11] M. Abdallah *et al.* [STAR], Phys. Rev. Lett. **127**, no.26, 262301 (2021)
[12] M. S. Abdallah *et al.* [STAR], Phys. Rev. Lett. **128**, no.20, 202303 (2022)
[13] [STAR], [arXiv:2207.09837 [nucl-ex]].
[14] W. j. Fu *et al.* , Phys. Rev. D **104**, 094047 (2021)
[15] B. Friman *et al.*, Eur. Phys. J. C **71** (2011), 1694
[16] P. Braun-Munzinger *et al.*, Nucl. Phys. A **1008**, 122141 (2021)
[17] X. Luo, J. Xu, B. Mohanty and N. Xu, J. Phys. G **40**, 105104 (2013)
[18] T. Nonaka, M. Kitazawa and S. Esumi, Phys. Rev. C **95**, no. 6, 064912 (2017)
[19] X. Luo, J. Phys. G **39**, 025008 (2012)
[20] A. Pandav, D. Mallick and B. Mohanty, Nucl. Phys. A **991**, 121608 (2019)
[21] STAR BES-II White paper [STAR], https://drupal.star.bnl.gov/STAR/starnotes/public/sn0598
[22] STAR Beam Use Request [STAR], https://drupal.star.bnl.gov/STAR/starnotes/public/sn0773